4. Izyumov Yu A, Kurmaev E Z *Phys. Usp.* **51** 1261 (2008); *Usp. Fiz. Nauk* **178** 1307 (2008)
5. Abrikosov A A *Physica C* **317–318** 154 (1999)
6. Fujioka M et al., arXiv:1401.5611
7. Klauss H-H et al. *Phys. Rev. Lett.* **101** 077005 (2008)
8. Mazin I I, Schmalian J *Physica C* **469** 614 (2009)
9. Liu R H et al. *Nature* **459** 64 (2009)
10. Boeri L, Dolgov O V, Golubov A A *Physica C* **469** 628 (2009)
11. Eliashberg G M *Sov. Phys. JETP* **11** 696 (1960); *Zh. Eksp. Teor. Fiz.* **38** 966 (1960)
12. Mazin I I et al. *Phys. Rev. Lett.* **101** 057003 (2008)
13. Korshunov M M, Eremin I *Phys. Rev. B* **78** 140509(R) (2008)
14. de la Cruz C et al. *Nature* **453** 899 (2008)
15. Paglione J, Greene R L *Nature Phys.* **6** 645 (2010)
16. Onari S, Kontani H *Phys. Rev. Lett.* **103** 177001 (2009)
17. Efremov D V et al. *Phys. Rev. B* **84** 180512(R) (2011)
18. Sato M et al. *J. Phys. Soc. Jpn.* **79** 014710 (2010)
19. Ikeuchi K et al. *JPS Conf. Proc.* **3** 015043 (2014)
20. Ishizuka J et al. *J. Phys. Soc. Jpn.* **82** 123712 (2013)
21. Shein I R, Ivanovskii A L *Phys. Lett. A* **375** 1028 (2011)
22. Pandey S, Chubukov A V, Khodas M *Phys. Rev. B* **88** 224505 (2013)
23. Zhou Y et al., arXiv:1311.0611
24. Kuchinskii E Z, Nekrasov I A, Sadovskii M V *JETP Lett.* **91** 518 (2010); *Pis'ma Zh. Eksp. Teor. Fiz.* **91** 567 (2010)
25. Zhigadlo N D et al. *Phys. Rev. B* **86** 214509 (2012)
26. Malone L et al. *Phys. Rev. B* **79** 140501(R) (2009)
27. Hashimoto K et al. *Phys. Rev. Lett.* **102** 017002 (2009)
28. Prakash J et al. *J. Phys. Condens. Matter* **21** 175705 (2009)
29. Chen G F et al. *Phys. Rev. Lett.* **101** 057007 (2008)
30. Mu G et al. *Chinese Phys. Lett.* **25** 2221 (2008)
31. Nakai Y et al. *Phys. Rev. B* **79** 212506 (2009)
32. Kawasaki S et al. *Phys. Rev. B* **78** 220506(R) (2008)
33. Matano K et al. *Europhys. Lett.* **83** 57001 (2008)
34. Yin Y et al. *Physica C* **469** 535 (2009)
35. Kondo T et al. *Phys. Rev. Lett.* **101** 147003 (2008)
36. Sato T et al. *J. Phys. Soc. Jpn.* **77** 063708 (2008)
37. Sugimoto A et al. *Physica C* **470** 1070 (2010)
38. Ekino T et al. *Physica C* **470** S358 (2010)
39. Jin R et al. *Supercond. Sci. Technol.* **23** 054005 (2010)
40. Fasano Y et al. *Phys. Rev. Lett.* **105** 167005 (2010)
41. Millo O et al. *Phys. Rev. B* **78** 092505 (2008)
42. Miyakawa N et al. *J. Supercond. Novel Magn.* **23** 575 (2010)
43. Tanaka M, Shimada D *J. Supercond. Novel Magn.* **24** 1491 (2011)
44. Samuely P et al. *Supercond. Sci. Technol.* **22** 014003 (2009)
45. Le Tacon M et al. *Phys. Rev. B* **78** 140505(R) (2008)
46. Seidel P *Supercond. Sci. Technol.* **24** 043001 (2011)
47. Stewart G R *Rev. Mod. Phys.* **83** 1589 (2011)
48. Daghero D et al. *Supercond. Sci. Technol.* **25** 084012 (2012)
49. Daghero D et al. *Rep. Prog. Phys.* **74** 124509 (2011)
50. Moskalenko V A *Fiz. Met. Metalloved.* **8** 503 (1959)
51. Moskalenko V A *Sov. Phys. Usp.* **17** 450 (1974); *Usp. Fiz. Nauk* **113** 340 (1974)
52. Suhl H, Matthias B T, Walker L R *Phys. Rev. Lett.* **3** 552 (1959)
53. Andreev A F *Sov. Phys. JETP* **19** 1228 (1964); *Zh. Eksp. Teor. Fiz.* **48** 1823 (1964)
54. Abrikosov A A et al. *Phys. Usp.* **53** 103 (2010); *Usp. Fiz. Nauk* **180** 109 (2010)
55. Sharvin Yu V *Sov. Phys. JETP* **21** 655 (1965); *Zh. Eksp. Teor. Fiz.* **48** 984 (1965)
56. Octavio M et al. *Phys. Rev. B* **27** 6739 (1983)
57. Flensberg K, Hansen J B, Octavio M *Phys. Rev. B* **38** 8707 (1988)
58. Arnold G B *J. Low Temp. Phys.* **68** 1 (1987)
59. Kümmel R, Gunsenheimer U, Nicolsky R *Phys. Rev. B* **42** 3992 (1990)
60. Ponomarev Ya G et al. *JETP Lett.* **79** 484 (2004); *Pis'ma Zh. Eksp. Teor. Fiz.* **79** 597 (2004)
61. Kuzmichev S A et al. *Solid State Commun.* **152** 119 (2012)
62. Moreland J, Ekin J W *J. Appl. Phys.* **58** 3888 (1985)
63. Ponomarev Ya G et al. *Phys. Rev. B* **79** 224517 (2009)
64. Ponomarev Ya G et al. *JETP* **113** 459 (2011); *Zh. Eksp. Teor. Fiz.* **140** 527 (2011)
65. Shanygina T E et al. *JETP Lett.* **93** 94 (2011); *Pis'ma Zh. Eksp. Teor. Fiz.* **93** 95 (2011)
66. Pudalov V M et al. *Phys. Usp.* **54** 648 (2011); *Usp. Fiz. Nauk* **181** 672 (2011)
67. Shanygina T E et al. *J. Phys. Conf. Ser.* **391** 012138 (2012)
68. Kuzmichev S A et al. *JETP Lett.* **95** 537 (2012); *Pis'ma Zh. Eksp. Teor. Fiz.* **95** 604 (2012)
69. Shanygina T E et al. *J. Supercond. Novel Magn.* **26** 2661 (2013)
70. Ponomarev Ya G et al. *J. Supercond. Novel Magn.* **26** 2867 (2013)
71. Kuzmicheva T E et al. *Europhys. Lett.* **102** 67006 (2013)
72. Kuzmichev S A et al. *JETP Lett.* **98** 722 (2013); *Pis'ma Zh. Eksp. Teor. Fiz.* **98** 816 (2013)
73. Chareev D et al. *CrystEngComm* **15** 1989 (2013)
74. Kuzmicheva T E, Kuzmichev S A, Zhigadlo N D *JETP Lett.* **99** 136 (2014); *Pis'ma Zh. Eksp. Teor. Fiz.* **99** 154 (2014)
75. Roslova M et al. *CrystEngComm* **16** 6919 (2014)
76. Ponomarev Ya G et al. *Physica C* **243** 167 (1995)
77. Aminov B A et al., in *Advances in Superconductivity V* (Eds Y Bando et al.) (Tokyo: Springer-Verlag, 1993) p. 1037
78. Ponomarev Ya G et al. *Inst. Phys. Conf. Ser.* (167) 241 (2000)
79. Ponomarev Ya G *Phys. Usp.* **45** 649 (2002); *Usp. Fiz. Nauk* **172** 705 (2002)
80. Nakamura H et al. *J. Phys. Soc. Jpn.* **78** 123712 (2009)
81. Khlybov E P et al. *JETP Lett.* **90** 387 (2009); *Pis'ma Zh. Eksp. Teor. Fiz.* **90** 429 (2009)
82. Zhigadlo N D et al. *Phys. Rev. B* **82** 064517 (2010)
83. Kondrat A et al. *Eur. Phys. J. B* **70** 461 (2009)
84. Yanson I K et al. *Phys. Rev. B* **67** 024517 (2003)
85. Wakimoto S et al. *J. Phys. Soc. Jpn.* **79** 074715 (2010)
86. Shamoto S-I et al. *Phys. Rev. B* **82** 172508 (2010)
87. Subedi A et al. *Phys. Rev. B* **78** 134514 (2008)
88. Kuzmichev S A, Kuzmicheva T E, Tchesnokov S N *JETP Lett.* **99** 295 (2014); *Pis'ma Zh. Eksp. Teor. Fiz.* **99** 339 (2014)

PACS numbers: **74.25.–q, 74.45.+c, 74.70.–b**
DOI: 10.3367/UFNe.0184.201408j.0897

Magnetic and transport properties of single crystals of Fe-based superconductors of the 122 family

Yu F Eltsev, K S Pervakov, V A Vlasenko, S Yu Gavrilkin, E P Khlybov, V M Pudalov

1. Introduction

Iron-based superconductors, just after their discovery in 2008 [1–5], have become a subject of great interest for the scientific community and occupy one of the leading places among the most topical subjects in contemporary solid-state physics [6, 7]. The present development of investigations of iron-containing superconductors can be compared perhaps with the great efforts to study properties of cuprate high-temperature

Yu F Eltsev, S Yu Gavrilkin Lebedev Physical Institute, Russian Academy of Sciences, Moscow, Russian Federation
E-mail: eltsev@sci.lebedev.ru
K S Pervakov, V A Vlasenko Lebedev Physical Institute, Russian Academy of Sciences, Moscow, Russian Federation; International Laboratory for Strong Magnetic Fields and Low Temperatures, Wroclaw, Poland
E P Khlybov Vereshchagin Institute of High-Pressure Physics, Russian Academy of Sciences, Troitsk, Moscow, Russian Federation; International Laboratory for Strong Magnetic Fields and Low Temperatures, Wroclaw, Poland
V M Pudalov Lebedev Physical Institute, Russian Academy of Sciences, Moscow, Russian Federation; Moscow Institute of Physics and Technology, Dolgoprudnyi, Moscow region, Russian Federation

Uspekhi Fizicheskikh Nauk **184** (8) 897–902 (2014)
DOI: 10.3367/UFNr.0184.201408j.0897
Translated by S N Gorin; edited by A Radzig

superconductors (HTSCs) in the first years after their discovery [8]. At present more than one hundred Fe-based superconductors of different compositions have been found. These compounds represent quite a new class of superconducting materials with crystal lattice containing ions of 3d metals (Fe, Co, Ni) well known as ferromagnetic metals. Therefore, *a priori*, other mechanism of superconducting pairing in Fe-based superconductors, different from the traditional electron–phonon coupling, cannot be ruled out. A characteristic feature of all iron-containing superconductors is the presence in their crystal structure of Fe–As layers in the case of pnictides or Fe–Se layers in the case of chalcogenides. At present, the maximum critical temperature T_c of the superconducting transition in Fe-based superconductors reaches 56 K [9] (in a $Gd_{1-x}Th_xFeAsO$ compound), which is inferior only to T_c of cuprate HTSCs. This circumstance undoubtedly makes it possible to place iron-based superconductors in the class of HTSCs.

Interest in iron-based superconductors is roused due to a whole number of fundamental and applied aspects. Firstly, the discovery of superconductivity in these compounds has broken the illusion that high-temperature superconductivity is exclusively a property of cuprate superconductors; secondly, it may be supposed that an investigation of the mechanism of high-temperature superconductivity in iron-containing superconductors will reveal ways of finding a more efficient mechanism of electron pairing than that existing in the cuprates and, correspondingly, can open the door to reaching higher values of T_c, which gives a new hope for the achievement of room-temperature superconductivity; thirdly, theoretical and experimental investigations of the energy-band structure of iron-containing superconductors yield values of the electron velocity v_F on the Fermi surface on the order of 10^6-10^7 cm s^{-1}, which, in turn, suggests small coherent lengths $\xi \sim \hbar v_F/2\pi k_B T_c \sim 1-3$ nm and, respectively, higher values of the upper critical field $H_{c2} = \phi_0/2\pi\xi^2$ exceeding 100 T [10]. Moreover, based on the experimental data, one can make an unambiguous conclusion that the density of the critical current in iron-containing superconductors at a liquid-helium temperature should exceed 10^6 A cm^{-2} [11–13], which is comparable with an analogous magnitude in cuprate superconductors. Iron-containing superconductors also possess a significantly smaller anisotropy of H_{c2} and J_c compared to cuprate superconductors [11], and the grain boundaries in these compounds, unlike those in cuprate superconductors, are 'transparent' to the superconducting current and do not restrict its magnitude [14]. All the above properties allow reaching a conclusion about the wide practicality of recently discovered iron-containing superconductors, primarily in 'strong-current' applications in high magnetic fields.

This report is not directed to an analysis of the existing concepts of the specific features of the band structure of iron-containing superconductors, possible mechanisms of superconducting pairing, types of symmetry of the order parameter, or the manifestation of multigap superconductivity. Rather, we focus our attention on the results (obtained by our team and other research groups) of investigations of the magnetotransport properties and current-carrying capacity of iron-containing superconductors, in particular, of $BaFe_{2-x}Ni_xAs_2$ crystals depending on the temperature, magnetic field, and the type of doping. This topic represents significant interest from the viewpoint of the estimation of the opportunity of practical applications of these materials.

2. Samples and measuring techniques

Optimally doped $BaFe_{2-x}Ni_xAs_2$ single crystals have lower values of T_c and $H_{c2}(0)$ than those of $Ba_{1-x}K_xFe_2As_2$ and $BaFe_{2-x}Co_xAs_2$ compounds of the 122 family, with the maximum critical temperatures reaching 40 and 25 K, respectively [14]. It might be possible that for this reason the crystals of the 122 family with an admixture of Ni have not been studied so intensely as the compounds of the 122 family doped with K and Co. On the other hand, the relatively low values of T_c and $H_{c2}(0)$ give a good opportunity to investigate the superconducting current-carrying properties and vortex pinning in $BaFe_2As_2$ single crystals doped with Ni in a wide temperature range covering almost the entire region of the phase diagram of this compound.

$BaFe_{2-x}Ni_xAs_2$ single crystals were grown by the self-flux method using as a flux a charge containing the components that enter the composition of the single crystals, in this case, FeAs. The starting components (Ba, FeAs, and NiAs) of high purity and with the total weight of ≈ 5 g were mixed in the molar proportion of $1:5(1-x):5x$, placed in a corundum crucible (3 cm^3 in volume), sealed in quartz tubes under a residual pressure of 0.2 atm of Ar, and placed into a tubular furnace. At the next step, the ampoule was heated to a temperature of 1200 °C, held at this temperature for 24 h (for the homogenization of the melt), and then cooled to 1070 °C at a rate of 2 °C h^{-1}. After having reached this temperature, the ampoule and the furnace were rotated from the vertical position by 90°–95° to sink the liquid flux from the crucible. Then, the ampoule with the crystals was cooled to room temperature together with the furnace. As a result, crystals were produced (almost free of flux) with dimensions of up to 4×2 mm^2 in the *ab*-plane with a thickness up to several hundred micrometers. The charaterization of the as-grown crystals using X-ray diffraction analysis has shown the absence of any foreign phase.

Figure 1a, where only peaks corresponding to $\{00l\}$ planes are seen, illustrates this conclusion for the $BaFe_{2-x}Ni_xAs_2$ samples with $x = 0.1$ and $x = 0.14$. The sample with the larger nickel concentration ($x = 0.14$) has a greater value of the lattice parameter along the *c*-axis. The decrease in the intensity of the reflections with increasing diffraction angle in the sample with $x = 0.1$ gives evidence of a somewhat inhomogeneous distribution of nickel over the crystal volume. The high perfection of the $BaFe_{2-x}Ni_xAs_2$ single crystals is also confirmed by the data given in Fig. 1b which demonstrates the temperature dependence of the real (χ') and imaginary (χ'') parts of the magnetic susceptibility for the sample with $x = 0.1$, measured in magnetic fields of 0, 1, 5, and 9 T applied along the *c*-axis.

It can be seen that in a zero magnetic field the width of the superconducting transition (estimated at the level of 10–90%) equals approximately 1.5 K; with increasing field, the transition is shifted toward lower temperatures and slightly broadens. The magnitude of T_c determined by extrapolation of the linear part of the susceptibility curve $\chi(T)$ to zero was 19.5 K. The estimation of the derivative of the upper critical field as a function of temperature yields $dH_{c2}/dT \approx -4.2$ T K^{-1}. From an analysis of similar data on $\chi'(T)$ for $BaFe_{1.86}Ni_{0.14}As_2$ crystals, the following values have been obtained: $T_c = 13$ K, and $dH_{c2}/dT \approx -3.6$ T K^{-1}.

To measure the magnetic and transport properties of grown crystals, samples of rectangular shape with dimensions of $\approx 2 \times (0.5-1.0) \times (0.1-0.2)$ mm^3 have been cleaved. The temperature dependence of the magnetic

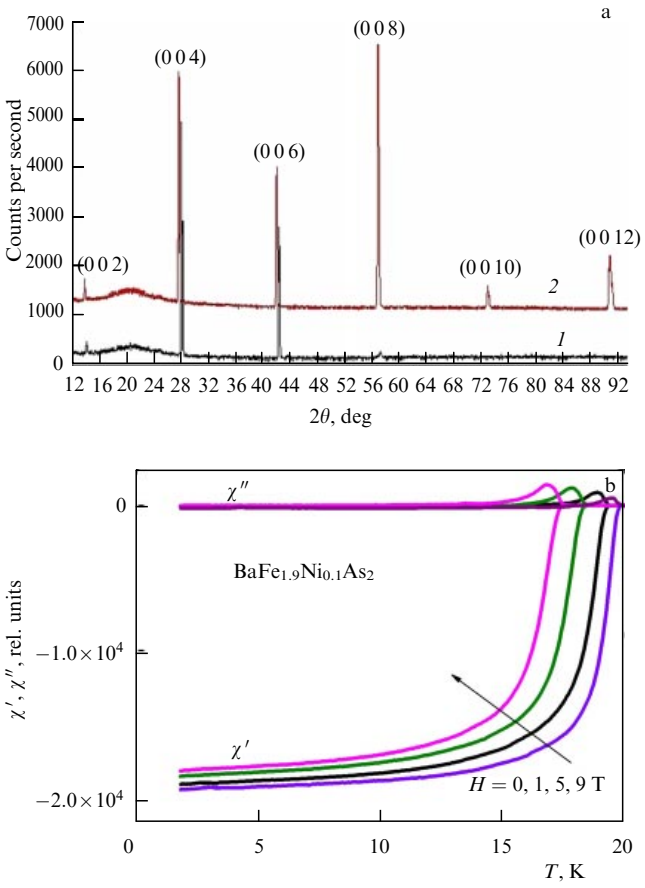

Figure 1. (a) Results of the X-ray phase diffraction analysis of (*1*) $BaFe_{1.9}Ni_{0.1}As_2$ and (*2*) $BaFe_{1.86}Ni_{0.14}As_2$ samples. (b) Temperature dependences of the real (χ') and imaginary (χ'') parts of the magnetic susceptibility for the $BaFe_{1.9}Ni_{0.1}As_2$ sample in magnetic fields of 0, 1, 5, and 9T applied along the *c*-axis [11].

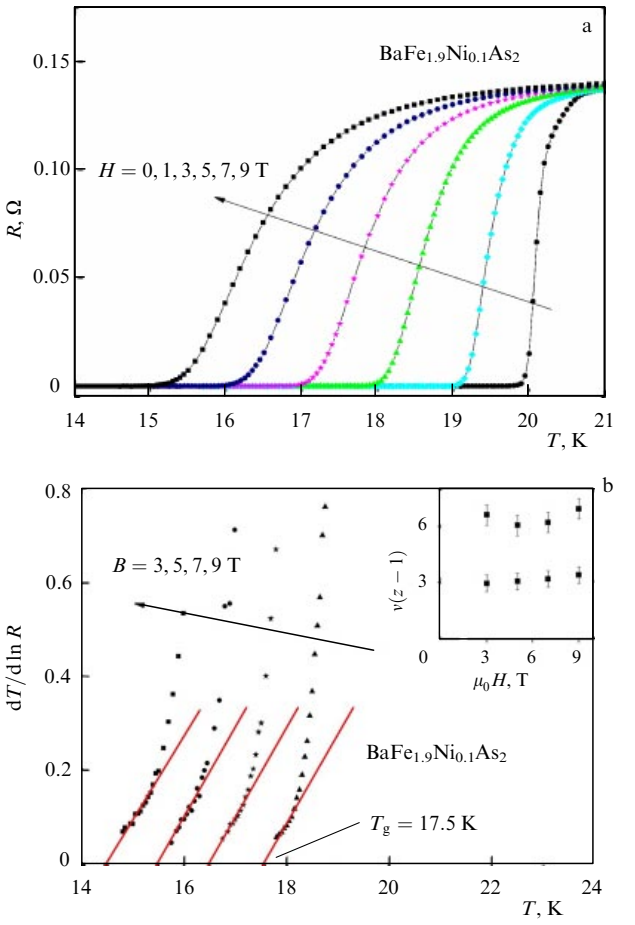

Figure 2. (a) Temperature dependence of the resistance of $BaFe_{1.9}Ni_{0.1}As_2$ crystal in different magnetic fields applied parallel to the *c*-axis of the crystal. (b) The $R(T)$ dependence of the $BaFe_{1.9}Ni_{0.1}As_2$ sample in different magnetic fields (indicated in the figure) in the Vogel–Fulcher coordinates. The straight line corresponds to the linear approximation of the experimental data. The arrow in the bottom part of the figure marks the melting point T_g of the vortex glass in the magnetic field of 3 T, obtained by linear extrapolation. The inset illustrates the dependence of the product of the critical exponents $\nu(z-1)$ on the magnetic field. The upper set of data points corresponds to the $BaFe_{1.9}Ni_{0.1}As_2$ sample, and the lower set to the $BaFe_{1.86}Ni_{0.14}As_2$ sample.

susceptibility was measured using a PPMS-9 (Physical Property Measurement System 9) (Quantum Design) facility. The measurements of the magnetization curves were performed using a low-frequency (3.6 Hz) vibration-sample magnetometer with a step motor [15] in the International Laboratory for Strong Magnetic Fields and Low Temperatures (Wroclaw, Poland). The typical rate of the magnetic-field sweep ranged within 20–90 Oe s^{-1}.

3. Magnetotransport properties of $BaFe_{2-x}Ni_xAs_2$ crystals ($x = 0.1$ and $x = 0.14$)

Figure 2a shows, as an example, the temperature dependence of the resistance $R(T)$ of a $BaFe_{1.9}Ni_{0.1}As_2$ crystal in magnetic fields of up to 9 T applied parallel to the *c*-axis. It can be seen that with increasing magnetic field the resistive superconducting transition is shifted toward lower temperatures, whereas its width remains almost unaltered. At small resistances near the onset of the superconducting transition, the temperature dependence of the resistance is described well in terms of the vortex glass model [16]: $R(T) \sim (T - T_g)^{n(z-1)}$, where T_g is the melting point of the vortex glass, and n and z are the static and dynamic critical exponents, respectively. This result is illustrated in Fig. 2b, where the $R(T)$ dependences are constructed in the Vogel–Fulcher coordinates. It can be seen that near the onset of the superconducting transition the derivative $(\mathrm{d}\ln R/\mathrm{d}T)^{-1}$ depends linearly on temperature. In this case, the $(\mathrm{d}\ln R/\mathrm{d}T)^{-1}$ straight lines as functions of temperature are extrapolated to the melting point (Fig. 2b). As can be seen from the inset to Fig. 2b, the slope of the $(\mathrm{d}\ln R/\mathrm{d}T)^{-1}$ straight lines as a function of T is independent of the magnitude of the applied magnetic field, also in agreement with the vortex glass model [16]. Similar data have also been obtained for $BaFe_{1.86}Ni_{0.14}As_2$ crystals. The only difference is lower melting points of the vortex glass T_g in this crystal.

One more evidence in favor of the applicability of the vortex glass model for the description of the magnetotransport properties of $BaFe_{2-x}Ni_xAs_2$ crystals are the results of measurements of the current–voltage (IV) characteristics). According to the vortex glass model [16], a positive curvature of the IV curves on the double logarithmic scale indicates the state of a liquid vortex glass, whereas a negative curvature of the IV characteristics corresponds to solid-state vortex glass with a nonzero critical current. A rectilinear IV characteristic in double logarithmic coordinates corresponds to the transition of the vortex system from the solid state to the liquid one.

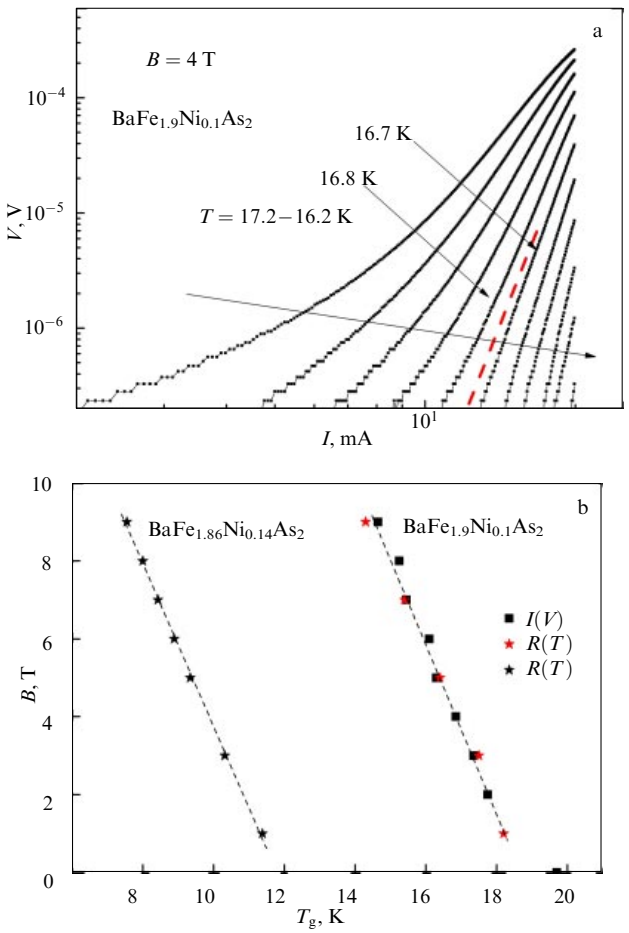

Figure 3. (a) Current–voltage characteristics of a $BaFe_{1.9}Ni_{0.1}As_2$ crystal in a magnetic field of 4 T at various temperatures with a step of 0.1 K. The dashed straight line corresponds to the melting point of the vortex glass, $T_g = 16.75$ K. (b) The melting curve $T_g(H)$ of the vortex-glass phase of $BaFe_{2-x}Ni_xAs_2$ crystals ($x = 0.1$ and $x = 0.14$). The asterisks correspond to the data obtained from $R(T)$ measurements, and squares are the data obtained from IV measurements.

In Fig. 3a, we give, as an illustration, the results of measurements of the IV curves for a $BaFe_{1.9}Ni_{0.1}As_2$ crystal in a magnetic field of 4 T at various temperatures with a step of 0.1 K. It can clearly be seen from the curves that at $T_g = 16.75$ K there is a change in the curvature of the IV characteristics from a positive to a negative curvature. Similar results have also been obtained for the other values of the applied magnetic field.

Thus, we can conclude on the base of the data obtained that the magnetotransport properties of $BaFe_{2-x}Ni_xAs_2$ crystals are described well by the vortex glass model. This conclusion is additionally illustrated by Fig. 3b, where we give the dependences of T_g on the magnetic field for $BaFe_{2-x}Ni_xAs_2$ crystal with $x = 0.1$ and 0.14, obtained from $R(T)$ measurements in various magnetic fields, as well as from CVCs measured in a fixed magnetic field at different temperatures. It is distinctly seen that these two independent methods of determining T_g give results that are in good agreement with each other.

4. Magnetic properties of $BaFe_{2-x}Ni_xAs_2$ crystals with $x = 0.1$ and $x = 0.14$ and peculiarities in the dependence of the critical current density on magnetic field

Figure 4 displays the results of measurements of the bulk isothermal irreversible magnetization $M(H)$ of $BaFe_{1.9}Ni_{0.1}As_2$ and $BaFe_{1.86}Ni_{0.14}As_2$ crystals depending on the magnetic field applied along the c-axis of the crystal (Figs 4a, 4b) and parallel to the ab plane (Figs 4c, 4d) at various temperatures indicated in the figures. The symmetry of the curves relative to the ordinate axis is clearly seen. In good agreement with the previously published data, the $M(H)$ curves also demonstrate a sharp peak near the zero magnetic field. In addition, for the $BaFe_{1.9}Ni_{0.1}As_2$ single crystal a second wide peak is observed in $J_c(H)$ for both orientations of the magnetic field, whereas for the $BaFe_{1.86}Ni_{0.14}As_2$ sample the second peak is absent. With increasing temperature, the position of the second peak is shifted toward lower magnetic fields. Notice that there is no common opinion on the nature of the second peak.

Based on the data presented in Fig. 4, we can calculate the critical current density in the crystals investigated, using the well-known expression $J_c = 20\Delta M/a(1 - a/3b)$ obtained in terms of the Bean model of the critical state [17, 18], where a and b $(b > a)$ are the crystal dimensions in the plane perpendicular to the applied magnetic field. As an example, we show in Fig. 5 the calculated critical current density for the $BaFe_{1.9}Ni_{0.1}As_2$ crystal depending on the field applied along the c-axis (Fig. 5a) and parallel to the ab plane (Fig. 5b) at various temperatures. As could be expected, in accordance with the data depicted in Fig. 4, the $J_c(H)$ dependence at all temperatures studied in the experiment is nonmonotonic with a wide peak which is shifted toward the lower fields with increasing temperature. In this case, the J_c value obtained at low temperatures exceeds 10^6 A cm^{-2}, which approaches the upper boundary of the previously published data on the critical current density in single crystals of the 122 family [14, 19–26].

The analysis of the dependence of the normalized pinning force $f_p = F_p/F_p^{max} = J_c(H)\,H/((J_c(H)\,H)_{max}$ on the normalized magnetic field $h = H/H_{c2}$ is a powerful tool for studying the mechanism of pinning in type-II superconductors. In the case of iron-containing compounds, just as in cuprate HTSCs, it is necessary to take into account that the region of the liquid vortex state occupies a significant part of the magnetic phase diagram and, respectively, the difference between the upper critical field and the irreversibility field is substantial. For this reason, it is expedient to use for the normalization of the applied magnetic field the irreversibility field H_{irr}, at which F_p and J_c become zero, instead of H_{c2}. In the Dew-Hughes model [27], the $f_p(h)$ curves obtained at various temperatures obey the scaling dependence $f_p \propto h^p(1-h)^q$ in the case of the single mechanism of pinning and should fall on a single curve with the identical position of the peak, which gives information on the nature of the pinning centers. The position of the peak at $h_{max} = 0.2$ suggests the pinning at grain boundaries; the position of the peak at $h_{max} = 0.33$ implies the pinning at normal point defects with dimensions on the order of the coherent length ξ, and, finally, the peak at $h_{max} = 0.7$ refers to the pinning caused by a spatial change of the order parameter. In the model developed by Kramer [28], the large density of strong pinning centers yields a clearly pronounced peak at low h, whereas the weak and rare pinning centers will give an $f_p(h)$ peak at higher h. Figure 6 displays the $f_p(h)$ dependence for $BaFe_{1.9}Ni_{0.1}As_2$ single crystals obtained at various temperatures in two orientations of the magnetic field using the data for $J_c(H)$ at temperatures covered in Fig. 5. The irreversibility field H_{irr} has been estimated using the data given in Fig. 4.

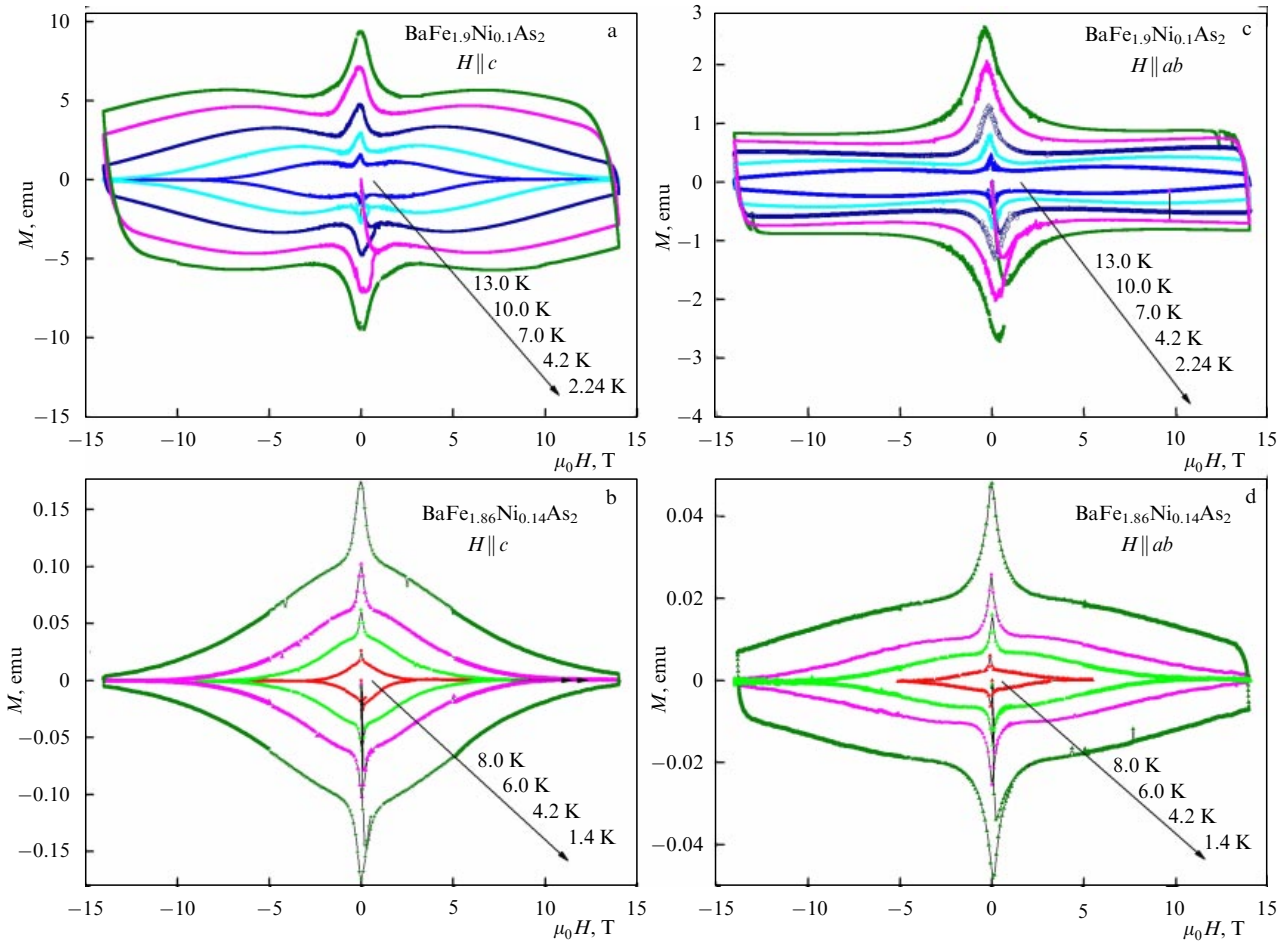

Figure 4. Isothermal irreversible magnetization M of $BaFe_{1.9}Ni_{0.1}As_2$ and $BaFe_{1.86}Ni_{0.14}As$ crystals at different temperatures (indicated in the figure) as a function of the magnetic field for two orientations of the magnetic field: $H \| c$, and $H \| ab$ [11].

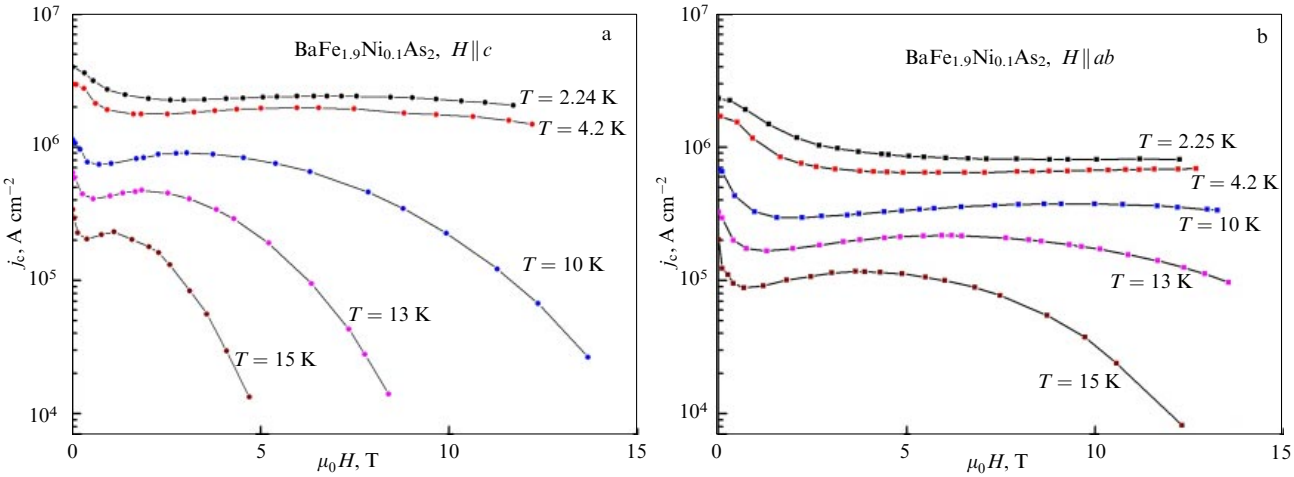

Figure 5. Critical current density for a $BaFe_{1.9}Ni_{0.1}As_2$ crystal depending on the magnetic field applied (a) along the c-axis, and (b) parallel to the ab plane at various temperatures [11].

Referring to Fig. 6, all experimental curves $f_p(h)$ within the scatter of the measurement fall on the same curve in the case of field orientation $H \| c$, which suggests a single mechanism of pinning (a similar result was obtained for a $BaFe_{1.86}Ni_{0.14}As_2$ sample with a greater nickel concentration). The scaling of the $f_p(h)$ curves was revealed in a wide temperature range 2–17 K; the scaling curve is described well by the expression $f_p(h) \sim h(1-h)^2$ with the peak position at $h_{max} \approx 0.3-0.4$, which, in accordance with the Dew-Hughes model [27], implies pinning on normal point defects. Our observation of the peaks at $h_{max} = 0.3-0.4$ agrees well with other experiments on crystals of the 122 family with hole and electron dopings, for which peaks were reported at $h_{max} = 0.32$, 0.37, and 0.43 [13, 24, 25]. As can be seen from Fig. 6, the curves measured in the field $H \| ab$ demonstrate a striking difference. In this case, the $f_p(h)$ curves reach their peaks at different points, thus demonstrating the absence of scaling. This result does not look surprising, since the

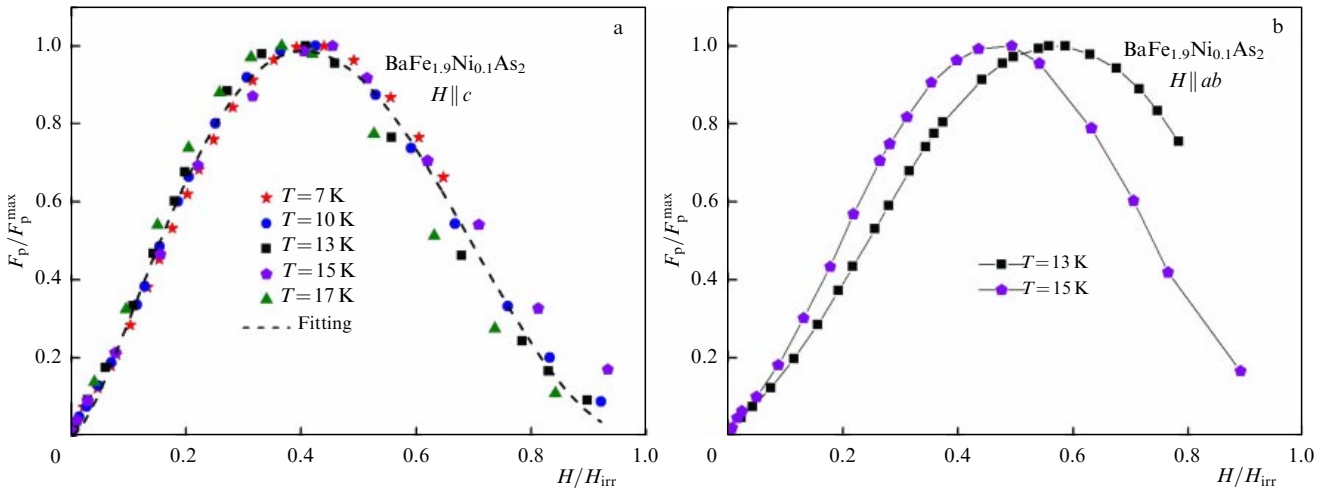

Figure 6. Dependences of the normalized pinning force $f_p = F_p/F_p^{max} = J_c(H)\,H/(J_c(H)\,H)_{max}$ on the normalized magnetic field $h = H/H_{irr}$ for $BaFe_{1.9}Ni_{0.1}As_2$ single crystals, measured at different temperatures for the orientations of the magnetic field (a) $H \| c$, and (b) $H \| ab$ [11].

screening current in the case of the magnetic field orientation parallel to the *ab*-plane consists of two components: a current flowing in the direction parallel to the *ab* planes, and a current directed parallel to the *c*-axis. These two components can be related to different mechanisms of pinning with different field and temperature dependences, which might explain the absence of scaling.

Acknowledgments

This work was partly supported by the Russian Foundation for Basic Research, project No. 13-02-01180. The authors are grateful to V P Martovitskii for carrying out the X-ray phase diffraction analysis of $BaFe_{1.9}Ni_{0.1}As_2$ and $BaFe_{1.86}Ni_{0.14}As_2$ crystals. The measurements of the magnetic and transport properties of the iron-containing crystals of the 122 family were performed using the equipment of the Center for Collaborative Access of the Lebedev Physical Institute, Russian Academy of Sciences, Moscow, Russia (in the framework of the theme "Investigations of Strongly Correlated Systems"), and of the International Laboratory for Strong Magnetic Fields and Low Temperatures, Wroclaw, Poland.

References

1. Kamihara Y et al. *J. Am. Chem. Soc.* **130** 3296 (2008)
2. Takahashi H et al. *Nature* **453** 376 (2008)
3. Zhi-An R et al. *Chinese Phys. Lett.* **25** 2215 (2008)
4. Rotter M, Tegel M, Johrendt D *Phys. Rev. Lett.* **101** 107006 (2008)
5. Wang X C et al. *Solid State Commun.* **148** 538 (2008)
6. Johnston D C *Adv. Phys.* **59** 803 (2010)
7. Paglione J, Greene R L *Nature Phys.* **6** 645 (2010)
8. U.S. Congress, Office of Technology Assessment, High-Temperature Superconductivity in Perspective, OTA-E-440 (Washington, DC: U.S. Government Printing Office, April 1990); http://ota.fas.org/reports/9024.pdf
9. Wang C et al. *Europhys. Lett.* **83** 67006 (2008)
10. Gurevich A *Rep. Prog. Phys.* **74** 124501 (2011)
11. Pervakov K S et al. *Supercond. Sci. Technol.* **26** 015008 (2013)
12. Pramanik A K et al. *J. Phys. Condens. Matter* **25** 495701 (2013)
13. Sun D L, Liu Y, Lin C T *Phys. Rev. B* **80** 144515 (2009)
14. Weiss J D et al. *Nature Mater.* **11** 682 (2012)
15. Nizhankovskii V I, Lugansky L B *Meas. Sci. Technol.* **18** 1533 (2007)
16. Fisher D S, Fisher M P A, Huse D A *Phys. Rev. B* **43** 130 (1991)
17. Bean C P *Phys. Rev. Lett.* **8** 250 (1962)
18. Bean C P *Rev. Mod. Phys.* **36** 31 (1964)
19. Fang L et al. *Phys. Rev. B* **84** 140504(R) (2011)
20. Shen B et al. *Phys. Rev. B* **81** 014503 (2010)
21. Haberkorn N et al. *Phys. Rev. B* **84** 094522 (2011)
22. Prozorov R et al. *Phys. Rev. B* **78** 224506 (2008)
23. Nakajima Y, Taen T, Tamegai T *J. Phys. Soc. Jpn.* **78** 023702 (2009)
24. Yamamoto A et al. *Appl. Phys. Lett.* **94** 062511 (2009)
25. Shahbazi M et al. *J. Appl. Phys.* **109** 07E151 (2011)
26. Wang X-L et al. *Phys. Rev. B* **82** 024525 (2010)
27. Dew-Hughes D *Philos. Mag.* **30** 293 (1974)
28. Kramer E J *J. Appl. Phys.* **44** 1360 (1973)